

# Poloidal Distribution Measurement of Inward Neutral Flux in LHD

Motoshi GOTO and Shigeru MORITA

*National Institute for Fusion Science, Toki 509-5292, Japan*

(Received 5 December 2006 / Accepted 12 March 2007)

Three emission lines of neutral helium, i.e., the  $\lambda$  667.8 nm ( $2^1\text{P}-3^1\text{D}$ ),  $\lambda$  728.1 nm ( $2^1\text{P}-3^1\text{S}$ ), and  $\lambda$  706.5 nm ( $2^3\text{P}-3^3\text{S}$ ) lines, are observed with an array of parallel lines-of-sight which covers an entire poloidal cross section of the plasma in the Large Helical Device (LHD). Their emission locations and intensities are determined from the Zeeman profiles. The electron temperature and density are evaluated from intensity ratios among the observed emission lines at each emission location and the poloidal distribution of ionization flux or its equivalent quantity, inward neutral particle flux, is derived with the help of collisional-radiative model calculations. A relatively strong neutral flux is observed at the inboard-side X-point and this result implies a high particle recycling in the inboard-side divertor region. The result is consistent with the ion flux distribution onto the helically located divertor plates measured with Langmuir probes.

© 2007 The Japan Society of Plasma Science and Nuclear Fusion Research

Keywords: spectroscopy, helium, Zeeman effect, collisional-radiative model

DOI: 10.1585/pfr.2.S1053

## 1. Introduction

A passive spectroscopic measurement with a collimated line-of-sight gives a line-integrated radiation intensity at the plasma edge, and it is generally difficult to determine the local structure of the emission location from such line-integrated data. In magnetically confined fusion plasmas, however, splittings of emission lines due to the Zeeman effect are helpful to determine their emission locations.

We have succeeded in a simultaneous measurement of the location and intensity of neutral helium emission lines over an entire poloidal cross section in the Large Helical Device (LHD) with the help of Zeeman splittings [1]. The results indicate that the helium emission region forms a narrow zone just outside the last closed flux surface (LCFS), and that the radiation intensity is relatively high in the vicinity of the inboard-side X-point.

Here, a question arises: what is the reason for such a localized strong radiation? The line emissions measured here are subject to the ionizing plasma and then its intensity can be a measure of the ionization flux [2]. Since the plasma is in a stationary state, the ionization flux is furthermore regarded as the inward atom flux. Therefore, the result in our previous study suggests an existence of strong inhomogeneity in the inward atom flux around the LHD plasma. The two-dimensional distribution measurement of the neutral flux is an important subject in relation to a recent study which points out an importance of poloidal neutral density variation for the transition to a high confinement mode in tokamaks [3].

Though a proportionality relationship has been assumed between the line intensity and ionization flux in our calculations, there really exists a slight dependence on the electron temperature  $T_e$  and electron density  $n_e$  [2]. Therefore, a measurement of these plasma parameters at each emission location is desired for a deeper understanding of the neutral particle behavior in the plasma edge region.

This paper presents our attempt on the  $T_e$  and  $n_e$  determination at each emission location which is based on the intensity ratio measurement among three emission lines of neutral helium [4, 5]. We encounter a difficulty in the analysis of the  $\lambda$  706.5 nm line out of the three lines required for the parameter determination: the energy levels related to the  $\lambda$  706.5 nm line belong to the triplet  $L$ - $S$  coupling scheme and the Zeeman effect is no longer expressed with a linear function while it is exactly valid for other two lines. Therefore, we solve the general problem of the Zeeman effect with the help of perturbation theory and use the results for the line profile fittings of the experimental data.

## 2. Zeeman Effect

For the measurement of  $T_e$  and  $n_e$ , intensity ratios among the  $\lambda$  728.1 nm ( $2^1\text{P}-3^1\text{S}$ ),  $\lambda$  667.8 nm ( $2^1\text{P}-3^1\text{D}$ ), and  $\lambda$  706.5 nm ( $2^3\text{P}-3^3\text{S}$ ) lines are used. The first two lines have been already found suitable for the method of the emission location determination in Ref. [1]. The  $\lambda$  706.5 nm line corresponds to the transition between triplet levels and the line splitting is no longer subject to the normal Zeeman effect which exhibits the so-called "Lorenz triplet". Though the upper state  $3^3\text{S}$  purely consists of a single fine structure level with  $J = 1$ , where  $J$  is the total

author's e-mail: goto@nifs.ac.jp

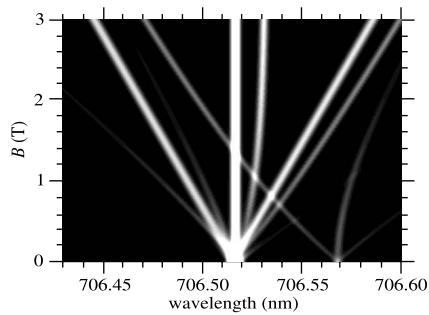


Fig. 1 Dependence on the magnetic field strength of the wavelength shifts for the HeI  $\lambda$  706.5 nm line.

angular momentum quantum number, and the level shifts are proportional to the strength of the magnetic field, the lower state  $2^3P$  has three fine structure levels with  $J = 0, 1,$  and  $2,$  and the intrinsic energy level separations between  $J = 0$  and the others are as large as the level shifts caused by the Zeeman effect with a typical magnetic field strength in LHD ( $\sim 3$  T). Consequently, the level splittings of the lower level and accordingly the emission line profile become so complicated that the general problem of the Zeeman effect must be solved.

The splittings and relative intensities of emission lines in a magnetic field are calculated in accordance with the perturbation theory. The energy levels are obtained as eigenvalues of the Hamiltonian which includes a perturbation term due to a magnetic field, and the line intensities or spontaneous transition probabilities between all pairs of magnetic sublevels involved in the upper and lower states are calculated from the wavefunctions which are also obtained as a solution of the eigenvalue problem.

Figure 1 shows the dependence on the magnetic field strength of the wavelength shifts and relative intensities among the split line components for the  $\lambda$  706.5 nm line. The brightness represents the relative intensity. Since the line splittings exhibit a rather complicated structure, the Lorenz triplet approximation is no longer applicable. This result is used in the analysis of observed line profiles as explained later.

### 3. Experiment

Emission lines are observed with 40 parallel viewing chords which cover an entire poloidal cross section of the plasma as shown in Fig. 2. Each line-of-sight is set up with a  $100\mu\text{m}$  diameter optical fiber and a collimator lens so that the spatial resolution is about 30 mm. The collected light is guided into an astigmatism-corrected Czerny-Turner type spectrometer (McPherson Model 209) [6] and the chord-resolved spectra are recorded on a CCD (charge coupled device) detector. The observation system is absolutely calibrated with a tungsten standard lamp.

The three emission lines required for the parameter determination are respectively measured in a series of

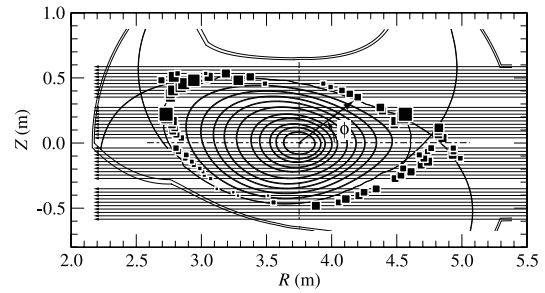


Fig. 2 Plasma cross section and viewing chords for the present observation. Emission locations for  $\lambda$  667.8 nm determined in the line profile analysis are also shown. The symbol size represents the intensity.

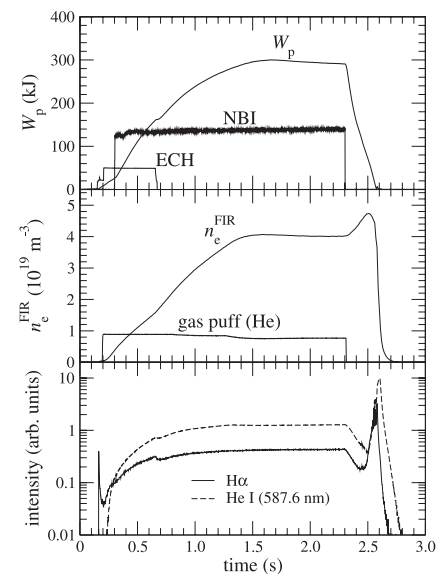


Fig. 3 Temporal development of a discharge for the present measurement with principal parameters.

almost identical three discharges with  $R_{\text{ax}} = 3.75$  m and  $B_{\text{ax}} = 2.64$  T, where  $R_{\text{ax}}$  is the magnetic axis radius and  $B_{\text{ax}}$  is the magnetic field strength on the magnetic axis. The temporal development of the discharge is shown in Fig. 3 with typical parameters. The spectra are acquired with a sampling rate of five frames per second, and they are summed over a stationary phase of the discharges from  $t = 1.6$  s to 2.2 s.

## 4. Results and Discussion

### 4.1 Profile analysis

Emission locations and intensities of the  $\lambda$  667.8 nm line are first determined with the same method as used in Ref. [1] except that the line width of all the narrow components is fixed to the instrumental width and the maximum number of Lorenz triplet components is limited to two. The former is justified by the fact that the line width is predominated by the instrumental width rather than by other physical broadening mechanisms. Due to the latter restric-

tion such cases that the  $\sigma$ -components are clearly broader than the  $\pi$ -component like Fig. 4 in Ref. [1] are excluded from the analysis. Figure 4 (a) shows an example of the fitting results. In this case values of 1.34 T and 1.82 T are derived as the field strength. A broad Gaussian component ( $\sim 14$  eV) has a fraction of about 18 % to the total intensity. Similar amount of broad component is found necessary in the fitting for most of the measured line profiles. The field strengths determined from the narrow line components are readily translated into spatial locations on the line-of-sight.

Since the total exposure time ( $\sim 0.6$  s) is shorter than that in the case of Ref. [1] ( $\sim 20$  s), the signal count of the  $\lambda 728.1$  nm line is sometimes too small to conduct an independent analysis. Therefore, we assume that (1) the emission locations and thereby the magnetic field strength values are the same as those derived from the  $\lambda 667.8$  nm line, and that (2) the relative velocities of neutral atoms between the inboard-side and outboard-side groups are the same as those derived from the  $\lambda 667.8$  nm line. Under these assumptions, only the amplitudes of the individual Lorentz triplet components are the independent parameters in the fitting of narrow components. The amplitude and width of a broad Gaussian component are also treated as independent parameters. Figure 4 (b) shows the fitting result of

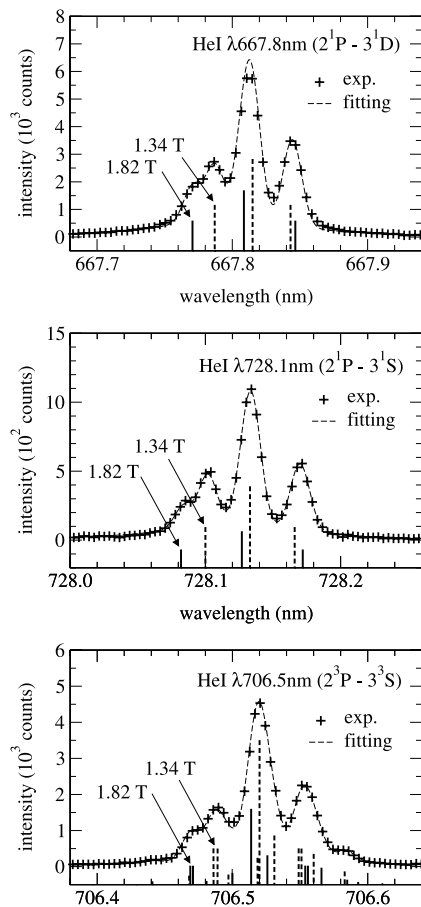


Fig. 4 Examples of line profile fitting for the (a)  $\lambda 667.8$  nm, (b)  $\lambda 706.5$  nm, and (c)  $\lambda 728.1$  nm lines of neutral helium.

the  $\lambda 728.1$  nm line for the same line-of-sight as taken for Fig. 4 (a).

For the  $\lambda 706.5$  nm line, the Lorentz triplet profile is no longer valid as seen in Fig. 1. Instead we calculate the line profile for a given field strength with the method introduced in Sec. 2. The experimental data are fitted with the superposition of two synthetic profiles and a broad Gaussian component. The same assumptions as for the case of the  $\lambda 728.1$  nm line are adopted, i.e., the field strength values and the relative velocities are taken from the fitting results for the  $\lambda 667.8$  nm line, and the amplitude and the width of the broad component are treated as independent parameters.

From the line profile fitting for all the lines-of-sight, the two-dimensional intensity distributions of the three emission lines are obtained. The result for the  $\lambda 667.8$  nm, for example, is shown in Fig. 2.

#### 4.2 $T_e$ and $n_e$ evaluation and inward neutral flux

The values of  $T_e$  and  $n_e$  are evaluated at each emission location with the same method as introduced in Ref. [5]. The results are shown in Fig. 5. Here, the abscissa represents the poloidal angle,  $\phi$ , which is defined as

$$\phi = \tan^{-1} \left( \frac{Z}{R - R_{ax}} \right), \quad (1)$$

where a set of  $Z$  and  $R$  values defines a location on the cross section in Fig. 2. It is found that the derived  $T_e$  values fall in a narrow range between 10 eV and 40 eV. As for the density, the difference between the highest and lowest values is about one order.

We define here a coefficient  $S_{CR}/\varepsilon$  as the ionization event number per a single photon emission. The ionization flux is derived as the product of this coefficient and the measured photon emission rate of the aimed emission line.

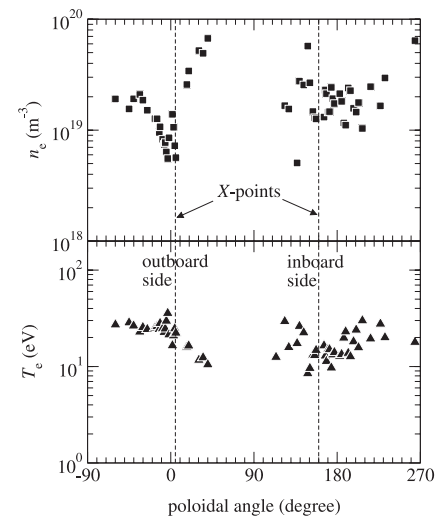


Fig. 5  $T_e$  and  $n_e$  distributions derived from intensity ratios of measured neutral helium lines.

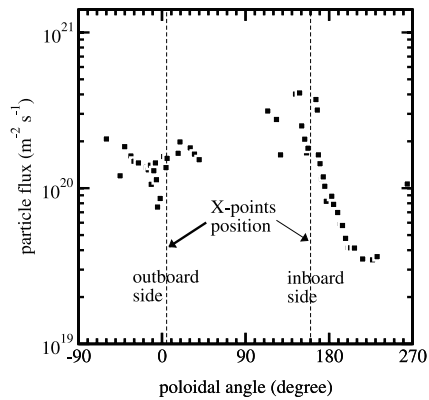


Fig. 6 Distribution of inward atom flux determined from emission line intensity of the  $\lambda$  667.8 nm line and derived  $T_e$  and  $n_e$  values.

When the plasma is in a stationary phase, the neutral atoms to be ionized must be replenished by the inward atom flux. Therefore, the ionization flux and the inward atom flux can be thought to be an equivalent quantity. Since the  $T_e$  dependence of the  $S_{CR}/\epsilon$  value is small in the temperature range derived here [2], the possibility that the poloidal inhomogeneity in the line intensity distribution is ascribed to the temperature variation is denied. The  $S_{CR}/\epsilon$  values for the  $\lambda$  667.8 nm line at respective emission locations are taken from Ref. [2] and the poloidal distribution of the inward particle flux is derived. The result is shown in Fig. 6.

In the vicinity of the inboard-side X-points, the distribution profile of the atom flux is similar to that of the emission line intensities as expected from the small variations of the plasma parameters, while the variation of the line intensities is compensated by  $n_e$  around the outboard-side X-point. The variation of the atom flux is consequently small. The increase in the atom flux at the inboard-side X-points implies a high particle recycling in the inboard-side divertor region. The Langmuir probe measurement shows high ion fluxes onto the inboard-side divertor plates [7]. This result tends to be consistent with the present results.

There are a few studies which predict the poloidal asymmetry of the neutral density distribution. Boivin et al. have calculated the density of neutral hydrogen at 5 mm inside the separatrix using DEGAS2 code for the Alcator C-Mod tokamak [8]. The highest neutral density appears at the inboard-side location on the midplane where the distance between the plasma and the vessel wall is the shortest, and the density is about one order higher than at

the X-point. The lowest and the highest densities are different by more than three orders. In Alcator C-Mod, the shortest distance between the plasma and the wall is about 2 cm, while that is longer than 20 cm in our observation at the location close to the helical coils. That might be a reason why we observe no intense radiation at this location. However, the distance between the plasma and the inboard-side wall is about 1 cm [9] at the vertically elongated plasma cross section. The particle recycling could be locally activated on the inboard-side wall surface and then the toroidally averaged neutral density would be higher in the inboard-side region than in the outboard-side region. If this is true, the higher neutral density at the inboard-side X-point as compared to that at the outboard-side X-point in our observation is understandable.

The reliability of the deduced parameters has yet to be assessed. Owing to the weak signals in the poloidal angle between 10 degrees and 40 degrees, the errors of the obtained parameters may be large in this region. It is noted for a reference that the change by a factor of two in the intensity ratio of the  $\lambda$  667.8 nm to  $\lambda$  728.1 nm lines corresponds to the change in  $n_e$  by about one order. Although a further detailed investigation is difficult at present, this method could be a powerful diagnostics tool for the poloidal inhomogeneity of the neutral particle flux in the plasma edge region.

## 5. Acknowledgment

This study has been made in part under the financial support by the LHD project (NIFS06ULPP527).

- [1] M. Goto and S. Morita, Phys. Rev. E **65**, 026401 (2002).
- [2] M. Goto, K. Sawada, and T. Fujimoto, Phys. Plasmas **9**, 4316 (2002).
- [3] T. Fülöp, P. Helander and Peter J. Catto, Phys. Rev. Lett. **89**, 225003 (2002).
- [4] B. Schweer, G. Mank, A. Pospieszczyk, B. Brosda, and B. Pohlmeier, J. Nucl. Mater. **196–198**, 174 (1992).
- [5] M. Goto, J. Quant. Spectrosc. Radiat. Transf. **76**, 331 (2003).
- [6] M. Goto and S. Morita, Rev. Sci. Instrum. **77**, 10F124 (2006).
- [7] S. Masuzaki, T. Morisaki, N. Ohya *et al.*, Nucl. Fusion **42**, 750 (2002).
- [8] R.L. Boivin, J.A. Goetz, A.E. Hubbard *et al.*, Phys. Plasmas **7**, 1919 (2000).
- [9] T. Morisaki, S. Sakakibara, K.Y. Watanabe *et al.*, Contrib. Plasma Phys. **40**, 266 (2000).